Magnitude of van der Waals—induced dipole moments in physisorption

Philippe Grossel
Laboratoire de Recherches Optiques, Faculté des Sciences, Université de Reims, Boîte Postale 347, 51062 Reims Cedex, France

Jean Marie Vigoureux
Laboratoire de Physique Moléculaire, Faculté des Sciences et des Techniques, la Bouloie, F-25030 Besancon Cedex, France

Daniel Van Labeke
Laboratoire de Recherches Optiques, Faculté des Sciences, Université de Reims, Boîte Postale 347, 51062 Reims Cedex, France
(Received 31 March 1986)

Near a surface an atom acquires a permanent electric dipole. When we take into account the presence of neighbors, three processes simultaneously contribute to the reduction of its dipole: a dipolar, a quadrupolar, and a quantum one. These depolarization processes of an adatom by its neighbors are particularly important for large coverage of the surface. We discuss them and give the expression for the dipole moment induced by such effects on an adatom. We then express the formulas with respect to the dipolar and quadrupolar polarizability and a nonlinear coefficient η, which leads us to propose numerical estimates of these effects for hydrogen and inert gases. For realistic distances of the adatom from the surface and from its neighbor, we show that the dipolar term has the greatest influence and that the quadrupolar-induced term always has a negligible influence on the neighboring adatom.

I. INTRODUCTION

It is well known that an important consequence of the interaction of an atom with a surface is the electric dispersive polarization of the initially symmetric atom. The appearance of such a static dipole moment has been for what may be the first time shown by Antoniewicz[1] and accurately restated by Linder and Kromhout[2,3] and Galatry and Girard[4,5] in the case of an adatom. We recently gave a presentation of this problem in the general case including retardation effects.[6,7] All these results are quite important to understand experimental results about adsorption. However, they are incomplete because they do not take into account cooperative effects between adatoms.

Our aim in this paper is then to study the depolarization of an adatom by its neighbors. This problem has been previously considered in a classical manner, for instance, by Topping[8] and Miller.[9] We show that three different processes contribute to the depolarization. The most important one arises from the static electric field (and from the static image field) of the permanent dipole induced on the neighboring atom by the surface. It varies as X^{-3} (X being the distance between the two adatoms) in the whole half-space, both in the short and in the long range. Numerical calculations for inert gases allow us to estimate this depolarization at about 5% when only one neighbor is considered. This result of course moves to higher values as the coverage of the surface is increased. Although this process is the most important, we also present two other processes which contribute to depolarization at the same order of perturbation: The first one can be understood as the effect of the static electric field (and of the static image field) of the quadrupole moment induced by the proximity of the surface on the neighbor. It is a static effect varying as X^{-4} whatever the distance between the two adatoms. The other process, more significantly, is a typical quantum effect. It varies as X^{-7} in the short range and as X^{-8} in the long range.

In these calculations we use quantum electrodynamic formalism as adopted in previous papers[6,7,10,11] to study interactions of electromagnetic radiation and matter or interactions between atoms or molecules near a surface. Although a similar formalism has been used by McLachlan[12] (for calculating the interaction energy) and by Babiker[13] (for studying energy transfer between adsorbed molecules), this method is not usually used in surface molecular physics. However, we think that it can give a clear description of surface phenomena (such as intermolecular forces, physisorption, light scattering, nonlinear effects, etc.) in a single theoretical framework. On the other hand, another advantage of this formalism is that, since the presence of the surface (with all characteristics of the solid half-space) is included in the definition of the propagator of the field, we may calculate all the possible interactions near the surface exactly as we do for a free field in vacuum. But for the final step when we must make the exact form of the propagator explicit, the results obtained in vacuum and near the surface are quite similar. This is helpful for anticipating and understanding surface effects.

Because of the above-noted remark and in order to sim-

plify the presentation of this paper, we restrict our study to atoms or centrosymmetric molecules near a Perfect metallic surface. It would be easy to generalize calculations to the case of a dispersive medium by modifying the field propagator appearing in final results. It is well known (Mavroyannis,[14] Galatry and Girard,[5] Schmeits and Lucas,[15] and Grossel[16]) that the consideration of a more realistic surface—free-electron gas—decreases image effects in a proportion of about 40%. This will then be taken into account in further numerical estimates.

We neglect exchange and overlap. Such effects have been studied by using the functional electronic density (Kohn and Sham[17] and Lang[18]), the charge-density susceptibilities (Linder and Kromhout[19]), or the nonlocal polarizability densities (Hunt[20]). Such calculations are quite general. However, since numerical expressions for the nonlocal polarizability are not known (except for hydrogen), calculations such as that presented in this paper remain useful. Our numerical estimations are given for inert-gas atoms for which such effects are less important. We also give numerical values for hydrogen. This atom has been extensively studied by Bruch and Ruijgrok[21] who used perturbation and variation methods to calculate the interaction energy and the induced dipole and quadrupole in the hydrogen-adsorbed ground state. Their leading term coincides with results presented in this paper.

II. PRESENTATION OF OUR FORMALISM

To begin this presentation of our formalism we note that, for purposes of comparing our results with those of other authors, some notations or even some definitions are not the same in the present paper as in our previous work. As explained in Sec. I we use quantum electrodynamic formalism as extended for interactions near surfaces in previous papers.[6,7,10,11]

In vacuum, calculations involving atoms or molecules interacting with one another or with a radiation field are generally simpler with the multipolar Hamiltonian than with the minimal coupling one. The connection between these two Hamiltonians can be performed by using a Power-Zienau transformation which may be used near a surface as recently shown by Power and Thirunamachandran.[22] With this multipolar Hamiltonian, interaction between two systems A and B are only mediated by transverse modes of the field. Consequently instantaneous Coulombic interactions do not explicitly appear provided we consider neutral systems.

We consider two systems A and B (atoms or molecules without any permanent electric dipole or quadrupole) located at the same distance d from the plane of a metallic surface and separated by a distance X (Fig. 1). Coordinates of A and B are then, respectively,

$$\mathbf{R}_A=(0,0,d) \quad \text{and} \quad \mathbf{R}_B=(X,0,d) \; .$$

We denote by $|f_A\rangle$ and $|f_B\rangle$ the fundamental states of the two systems and $|e_A\rangle, |e'_A\rangle, \ldots, |e_B\rangle, |e'_B\rangle, \ldots$ their respective excited states. Energies of these states are written $E_f, E_e, E_{e'}, \ldots$, respectively.

The Feynman propagator D^F_{ij} of the electromagnetic mode (in the presence of the surface) between two time-space points $(\mathbf{R}_A,\tau_A)$ and $(\mathbf{R}_B,\tau_B)$ was defined in Ref. 6. With $R_{AB}=|\mathbf{R}_B-\mathbf{R}_A|$ and $\tilde{R}_{AB}=|\mathbf{R}_B-\mathbf{R}_{\tilde{A}}|$, where $\tilde{A}$ is the image of A in the mirror, we have

$$D^F_{ij}(\mathbf{R}_A,\tau_A,\mathbf{R}_B,\tau_B)=-\frac{1}{2}\frac{i\hbar c}{(2\pi)^2\epsilon_0}\int_{-\infty}^{+\infty} dk_0 \exp[-ick_0(\tau_B-\tau_A)][g^F_{ij}(k_0,R_{AB})+\Theta_i g^F_{ij}(k_0,\tilde{R}_{AB})] \; , \tag{1}$$

where Θ_i is the reflection coefficient of the perfect mirror

$$\Theta_i=-1 \quad \text{for } i=x \text{ or } y; \quad \Theta_i=1 \quad \text{for } i=z$$

and g^F_{ij} is the Fourier transform of the Feynman propagator of the free field in vacuum,

$$g^F_{ij}(k_0,R)=e^{i|k_0|R}|k_0|^3\left[\frac{1}{|k_0|R}\left[\delta_{ij}-\frac{R_iR_j}{R^2}\right]+\left[\frac{i}{|k_0|^2R^2}-\frac{1}{|k_0|^3R^3}\right]\left[\delta_{ij}-3\frac{R_iR_j}{R^2}\right]\right] . \tag{2}$$

The use of this propagator takes into account retardation effects (see, for instance, Ref. 6). This formalism is thus valid whatever the distance between A, B, and the surface; that is to say, both at the long range (physisorption) and at the very long range.

The multipolar Hamiltonian that we use here is (in the 0-spin approximation)

$$H=-\boldsymbol{\mu}^A\cdot\mathbf{E}(\mathbf{R}_A)-\tfrac{1}{3}\overleftrightarrow{Q}^A:\nabla\cdot\mathbf{E}(\mathbf{R}_A)-\mathbf{M}^A\cdot\mathbf{B}(\mathbf{R}_A)+(A\leftrightarrow B) \; , \tag{3}$$

with

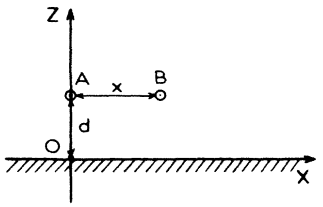

FIG. 1. Frame of reference for our calculations. The two systems A and B are placed at points $(0,0,d)$ and $(X,0,d)$, respectively. The x axis is directed from A towards B.

$$Q_{ij}^{A}=\sum_{\alpha}-\tfrac{3}{2}e(r_{\alpha i}r_{\alpha j}-\tfrac{1}{3}r_{\alpha}^{2}\delta_{ij})\ . \tag{4}$$

$\mu^{A(B)}$,$\overleftrightarrow{Q}^{A(B)}$,$\mathbf{M}^{A(B)}$ are the dipolar electric, quadrupolar electric, and dipolar magnetic moments of the system A (B). In order to calculate the dipole and quadrupole induced by the surface we use a fictitious external static field that we note as $\mathbf{E}^{s}$. Let us point out that, for effects considered in this paper, magnetic terms can be neglected in Eq. (3) because of the symmetry of the field propagator.

To calculate explicitly and to illustrate clearly the depolarizing processes we use Feynman diagrams. In such diagrams (see, for example, Fig. 2) we choose to represent electric dipole and quadrupole vertices by ○ and □, respectively.

Horizontal lines represent external static fields and wavy lines correspond to virtual modes of the electromagnetic field near the surface. As explained in Ref. 6, we emphasize here that, because the interface is included in the definition of the electromagnetic modes, calculations are to be performed exactly as we do in a free field in vacuum. In other words, internal photon lines take into account all specific surface effects.

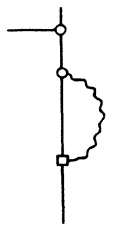

FIG. 2. Graph illustrating the appearance of a permanent electric dipole induced on the system by the surface. ○ and □ indicate a dipolar and a quadrupolar interaction, respectively; the wavy line corresponds to a virtual mode of the electromagnetic field near the surface. Horizontal lines correspond to a static electric field.

III. ATOMIC DEFORMATION INDUCED BY A SURFACE

A first important consequence of the interaction of an atom and a surface is the appearance on the adatom of a permanent electric dipole. At the same order of perturbation, another effect necessary to understand the atomic deformation induced by the surface is the appearance of a quadrupole moment. As far as we know, this effect was calculated for the first time by Grossel, Van Labeke, and Vigoureux.[7]

To make explicit the depolarization of an adatom by its neighbor we need the expressions of these surface-induced dipole and quadrupole moments. Consequently we summarize here the principal results concerning these two effects. To do this we refer to the papers of Refs. 6 and 7 and, as explained above, we seize the opportunity to modify some of our previous notations.

As explained in Ref. 6, the dipole moment μ of the system can be obtained by differentiating the interaction energy ΔU with respect to an external fictitious static field $\mathbf{E}^{s}$,

$$\mu_{l}=-\frac{\partial}{\partial E_{l}^{s}}\Delta U\ . \tag{5}$$

In the lowest order, ΔU can be evaluated by adding contributions of all the Feynman diagrams similar to the one presented in Fig. 2.

As calculated in Ref. 6, we thus obtain the expression for the dipole moment induced on the atom by the surface,

$$\mu_{l}=\frac{1}{4\pi\epsilon_{0}}\frac{\hbar c}{6\pi}\sum_{i,j,k}(1+\Theta_{i}\Theta_{j}\Theta_{k})\Theta_{j}\partial_{i}\times\int_{0}^{\infty}du\,g_{jk}^{F}(iu,\tilde{R})\chi_{lk,ij}(0,iu)\ . \tag{6}$$

Let us note that the difference between this result and that of Ref. 6 only arises from the definition of $\chi(0,iu)$ that we express in the present work in terms of the quadrupolar electric moment given in Eq. (4),

$$\begin{aligned}\chi_{lk,ij}(0,iu)=\sum_{i,j}\Bigg[&\langle f\,|\,\mu_{l}\,|\,e'\rangle\langle e'\,|\,\mu_{k}\,|\,e\rangle\langle e\,|\,\Theta_{ij}\,|\,f\rangle\\&\times\frac{1}{E_{e'}-E_{f}-i\eta}\left[\frac{1}{E_{e}-E_{f}-i\eta+i\hbar cu}+\frac{1}{E_{e}-E_{f}-i\eta-i\hbar cu}\right]\\&+\langle f\,|\,\mu_{l}\,|\,e'\rangle\langle e'\,|\,\Theta_{ij}\,|\,e\rangle\langle e\,|\,\mu_{k}\,|\,f\rangle\frac{1}{E_{e'}-E_{f}-i\eta}\left[\frac{1}{E_{e}-E_{f}-i\eta+i\hbar cu}+\frac{1}{E_{e}-E_{f}-i\eta-i\hbar cu}\right]\\&+\langle f\,|\,\mu_{k}\,|\,e'\rangle\langle e'\,|\,\mu_{l}\,|\,e\rangle\langle e\,|\,\Theta_{ij}\,|\,f\rangle\left[\frac{1}{(E_{e'}-E_{f}-i\eta+i\hbar cu)(E_{e}-E_{f}-i\eta+i\hbar cu)}\right.\\&\left.+\frac{1}{(E_{e'}-E_{f}-i\eta-i\hbar cu)(E_{e}-E_{f}-i\eta-i\hbar cu)}\right]\Bigg]\ .\end{aligned} \tag{7}$$

In a similar way we can calculate the permanent quadrupolar moment

$$Q_{kl}=-3\frac{\partial\Delta U}{\partial(\partial_k E_l^s)} \tag{8}$$

induced on the atom by the surface by using all permutations of Feynman diagrams presented in Fig. 3 (see Ref. 7). We thus obtain

$$Q_{kl}=\frac{1}{4\pi\epsilon_0}\frac{\hbar c}{4\pi}\sum_{i,j}(\Theta_i+\Theta_j)\int_0^\infty du\, g_{ij}^F(iu,\tilde{R})\chi'_{lk,ij}(0,iu)\ , \tag{9}$$

with

$$\begin{aligned}\chi'_{lk,ij}(0,iu)=\sum_{e,e'}\Bigg[&2\langle f\,|\,\Theta_{lk}\,|\,e'\rangle\langle e'\,|\,\mu_j\,|\,e\rangle\langle e\,|\,\mu_i\,|\,f\rangle\\&\times\frac{1}{E_{e'}-E_f-i\eta}\left[\frac{1}{E_e-E_f-i\eta+i\hbar cu}+\frac{1}{E_e-E_f-i\eta-i\hbar cu}\right]\\&+\langle f\,|\,\mu_j\,|\,e'\rangle\langle e'\,|\,\Theta_{lk}\,|\,e\rangle\langle e\,|\,\mu_i\,|\,f\rangle\\&\times\left[\frac{1}{(E_e-E_f-i\eta+i\hbar cu)(E_{e'}-E_f-i\eta+i\hbar cu)}\right.\\&\left.+\frac{1}{(E_e-E_f-i\eta-i\hbar cu)(E_{e'}-E_f-i\eta-i\hbar cu)}\right]\Bigg]\ .\end{aligned} \tag{10}$$

Results given in Eqs. (6) and (9) are quite general and include retardation effects. We give their expressions in the near zone where the propagator (2) can be restricted to its only last term,

$$g_{ij}^F(k_0,\tilde{R})=-\frac{1}{\tilde{R}^3}\left[\delta_{ij}-3\frac{\tilde{R}_i\tilde{R}_j}{\tilde{R}^2}\right]\ . \tag{11}$$

If the species is spherically symmetric we also have [both for Eqs. (7) and (10)]

$$\chi^{(\prime)}_{lk,ij}(0,iu)=\chi^{(\prime)}(0,iu)\left(-\tfrac{1}{2}\delta_{ij}\delta_{kl}+\tfrac{3}{4}\delta_{ik}\delta_{jl}+\tfrac{3}{4}\delta_{il}\delta_{jk}\right)\ . \tag{12}$$

By inserting Eqs. (11) and (12) into Eqs. (6) and (9) we get the nonretarded (electrostatic limit) results

$$\mu_x=\mu_y=0,\quad \mu_z=-\frac{1}{4\pi\epsilon_0}\frac{3\hbar c}{8\pi}\frac{1}{d^4}\int_0^\infty du\,\chi(0,iu)\ , \tag{13}$$

$$Q_{xx}=Q_{yy}=-\tfrac{1}{2}Q_{zz}=-\frac{1}{4\pi\epsilon_0}\frac{\hbar c}{32\pi}\frac{1}{d^3}\int_0^\infty du\,\chi'(0,iu)\ . \tag{14}$$

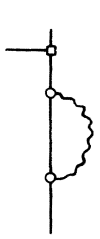

FIG. 3. Graph illustrating the appearance of a permanent electric quadrupole induced on the system by the surface.

Equations (13) and (14) give a picture of the deformation induced in the atom by the surface: Because of the existence of an attractive potential energy between the atom and the surface, the spherical electronic cloud of the atom is attracted towards the surface and the centers of gravity of the positive and negative charges are then separated ($\mu_z>0$). Another consequence just as important as the first one is the deformation of the initially spherical cloud: Near the surface the atom is not now spherical but looks like an ellipsoid whose major axis is perpendicular to the surface ($Q_{zz}=-2Q_{xx}=-2Q_{yy}<0$).

Noting

$$\alpha_Q=\sum_n{}'2\frac{|\langle f\,|\,\Theta_{zz}\,|\,n\rangle|^2}{E_{nf}} \tag{15}$$

TABLE I. Numerical calculation for the permanent dipole moment induced on the atom by the surface. These results correspond to the case of a perfect metallic surface and use formula (17). The nonlinear coefficient η has been taken from Ref. 24. Let us emphasize here that the value of η for Xe cannot be found in the literature. The value $\eta=150$ used in this table is thus our own estimate.

	η Ref. 24 (a.u)	$\mu_z d^4$ (a.u)	$\mu_z d^4$ (D Å^4)
H	16.5	6.19	1.22
He	2.525	0.95	0.19
Ne	8.617	3.23	0.64
Ar	39.21	14.70	2.90
Kr	73.06	27.40	5.46
Xe	(150)	(56)	(11)

TABLE II. Numerical calculation for the quadrupolar moment induced on the atom by the surface. Let us recall that $Q_{zz}=-2Q_{xx}=-2Q_{yy}$. Formula (18) has been used and the quadrupolar polarizability α_Q was found in Ref. 25.

	α_Q Ref. 25 (a.u.)	$Q_{zz}d^3$ (a.u.)	$Q_{zz}d^3$ (10^{-40} C m^2)
H	15	−0.62	−0.42
He	2.44	−0.10	−0.07
Ne	6.42	−0.27	−0.18
Ar	50.21	−2.01	−1.38
Kr	95.55	−3.98	−2.64
Xe	212.6	−8.85	−5.88

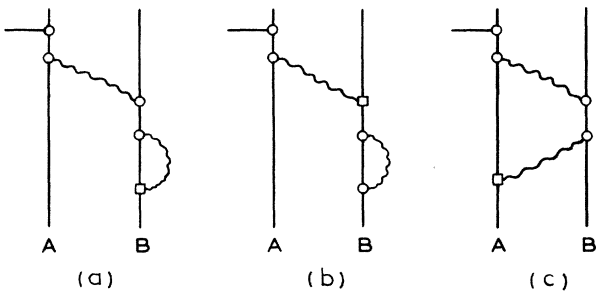

FIG. 4. Graph illustrating the modification the permanent-induced dipole of the system A by the proximity of the system B. (a), (b), and (c) illustrate the three different effects discussed in the text.

(the prime indicates that the ground state $|f\rangle$ is excluded from the summation), and introducing the η coefficient of Byers Brown and Whisnant[23,24]

$$\eta=\frac{-1}{\pi}\int_0^\infty du\,\chi(0,iu)\,, \tag{16}$$

results (13) and (14) can be written

$$\mu_z=\frac{3\eta}{8}ea_0\left[\frac{a_0}{d}\right]^4, \tag{17}$$

$$Q_{zz}=-\tfrac{1}{24}\alpha_Q ea_0^2\left[\frac{a_0}{d}\right]^3. \tag{18}$$

In the above results, e and a_0 are the proton charge and the Bohr radius, respectively. Using numerical estimations of Byers Brown and Whisnant[23] we obtain in the case of the hydrogen atom

$$\mu_z=6.19ea_0\left[\frac{a_0}{d}\right]^4, \tag{19}$$

$$Q_{zz}=-0.625ea_0^2\left[\frac{a_0}{d}\right]^3. \tag{20}$$

For hydrogen atoms the above-noted results coincide with those of Bruch and Ruijgrok.[21]

Numerical estimates for inert gases are given in Tables I and II (Ref. 25).

IV. van der WAALS INTERACTIONS BETWEEN ADATOMS

Sinanoglu and Pitzer[26] showed that the vicinity of a surface strongly modifies van der Waals forces between two systems. Our aim, now, is to show that in a quite similar manner, the surface modifies the permanent dipole [Eqs. (6), (13), and (17)] of each adatom.

To calculate this effect we proceed exactly as Vigoureux[27] did in calculating the static dipole moment of two coupled atoms. The dipole moment μ_A of A can be obtained, as in Eq. (5), by differentiating the energy shift of the coupled system with respect to a fictitious external static field. In the case where the two coupled systems are atoms (or spherical molecules) the parity selection rules show that ΔU can be obtained in the lowest order from graphs of Fig. 4 (we do not represent there the additional graphs which only differ by all the possible different positions of the quadrupole and dipole vertices).

As expected, three quite different graphs (and thus three different processes) contribute to the reduction of the permanent dipole of the adatom by the neighbor. The first one is illustrated by Fig. 4(a). Its physical meaning becomes clear when we identify the graph of Fig. 2 as a part of that in Fig. 4(a): This process corresponds to the polarization of the atom A by the static electric field of the permanent dipole μ^B (induced on B by the surface) [Fig. 5(a)] and of its image [Fig. 5(b)].

In the same way, Fig. 4(b) (in which we identify Fig. 3) corresponds to the polarization of A by the static field of the permanent quadrupole (induced on B by the surface) and of the image quadrupole. The last graph in Fig. 4(c) is an irreducible diagram which cannot be separated (as the two first) into two distinct physical processes: one acting on A and the other on B. To be brief, in Sec. IV A we call it the "quantum contribution" to polarization.

In order to calculate ΔU we have to add contributions of all these diagrams. However, to be clearer in further discussions we consider successively these three different effects.

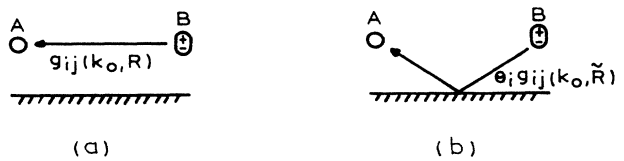

FIG. 5. Schematical representation of the polarization of system A by the induced deformation of system B. (a) indicates the direct influence of B on A; (b) indicates the image influence of B on A.

A. Depolarization of A by the static dipole induced on B by the surface

This first effect is described by 12 different graphs obtained from the graph in Fig. 4(a) by permuting different vertices. Given these diagrams one can immediately write down the corresponding matrix element. We shall not dwell on this graphical method at this point since it is lucidly set forth in Refs. 6 and 7 where we set forth in detail expressions associated with each external and internal atomic lines, internal photonic terms, and vertices.

The essential feature of this calculation is as follows: When integrating on all possible electromagnetic modes, $\mathbf{k}'$ exchanged between A and B, only the zero-frequency mode ($\mathbf{k}'=\mathbf{0}$) gives a nonzero contribution to ΔU. Substituting this value ($|k'|=0$) into Eq. (2) it is clear that the field propagator reduces to its only last term (11) not only in the near zone (London zone) but also in the whole half-space (Fig. 6). Its R-dependent part is thus varying as R^{-3} without approximation whatever the distance between the two adatoms.

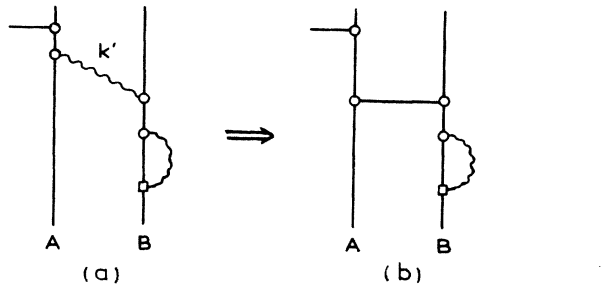

FIG. 6. Resulting graph. Only the $\mathbf{k}'=0$ mode has a nonzero contribution: The static electric field of the induced dipole B polarizes the system A.

Taking the above-noted remark into account, we find for the contribution of the graph in Fig. 4(a) to ΔU,

$$\Delta U_{(a)}=-\frac{1}{16\pi^2\epsilon_0^2}\frac{\hbar c}{6\pi}\sum_{i,j,k,l}\sum_{\alpha,\beta}E^s_\beta[g^F_{\alpha l}(0,R_{BA})+\Theta_\alpha g^F_{\alpha l}(0,\tilde{R}_{BA})]$$
$$\times\alpha^A_{\alpha\beta}(0)\int_0^\infty du\,\chi^B_{lk,ij}(0,iu)(1+\Theta_i\Theta_j\Theta_k)\Theta_j\partial^B_i[g^F_{jk}(iu,\tilde{R}_B)]\,, \tag{21}$$

where $\alpha^A_{\alpha\beta}(0)$ is the static polarizability of system A,

$$\alpha^A_{\alpha\beta}(0)=2\sum_e\frac{\langle f|\mu_\alpha|e\rangle\langle e|\mu_B|f\rangle}{E_e-E_f}\,. \tag{22}$$

Using then in Eq. (6) the contribution of both the static dipole μ_B (induced on B by the surface), and of its image to the dipole moment of A, we have

$$\mu_B^{A\leftarrow(a)}=-\frac{\partial}{\partial E^s_\rho}\Delta u_{(a)}=\frac{1}{4\pi\epsilon_0}\sum_{l,\alpha}\mu^B_l[g^F_{\alpha l}(0,R_{BA})+\Theta_\alpha g^F_{\alpha l}(0,\tilde{R}_{BA})]\alpha^A_{\alpha\beta}(0)\,. \tag{23}$$

Introducing expression (2) of the propagator in the particular case $|k_0|\equiv 0$ into this result we get

$$\mu_\beta^{A\leftarrow(a)}=-\frac{1}{4\pi\epsilon_0}\sum_{l,\alpha}\mu^\beta_l\alpha^A_{\alpha\beta}(0)\left[\frac{1}{R^3}\left[\delta_{l\alpha}-\frac{3R_lR_\alpha}{R^2}\right]+\frac{1}{\tilde{R}^3}\left[\delta_{l\alpha}-\frac{3\tilde{R}_l\tilde{R}_\alpha}{\tilde{R}^2}\right]\right]. \tag{24}$$

As shown in Fig. 1 the distances $R=R_{BA}$ between A and B and $\tilde{R}=\tilde{R}_{BA}$ between A and the image of B can be written

$$\mathbf{R}=(X,0,0),\quad R=X\,,$$
$$\tilde{\mathbf{R}}=(X,0,2d),\quad \tilde{R}=(X^2+4d^2)^{1/2}\,, \tag{25}$$

respectively. Using then Eq. (25) and taking into account that for a spherically symmetric system $[\alpha_{xx}(0)=\alpha_{yy}(0)=\alpha_{zz}(0)=\alpha]$

$$\alpha_{\alpha\beta}(0)=\alpha\delta_{\alpha\beta}\,, \tag{26}$$

Eq. (24) leads to

$$\mu_x^{A\leftarrow(a)}=-\frac{1}{4\pi\epsilon_0}\alpha^A\mu^B_z(d)\left[\frac{6Xd}{(X^2+4d^2)^{5/2}}\right],$$
$$\mu_z^{A\leftarrow(a)}=\frac{1}{4\pi\epsilon_0}\alpha^A\mu^B_z(d)\left[-\frac{1}{X^3}+\frac{8d^2-X^2}{(X^2+4d^2)^{5/2}}\right]. \tag{27}$$

It can easily be shown that in Eq. (27), for μ_z, the term in parentheses is negative whatever the values of X and d. The calculated effect is then always a *depolarizing* one.

If A and B are two identical adatoms in contact with both the surface and with one another, we have (d is then the radius of the adatom)

$$R=X=2,$$
$$\tilde{R}=(X^2+4d^2)^{1/2}=8^{1/2}d\ , \tag{28}$$

and Eq. (27) becomes

$$\mu_x^{A\leftarrow(a)}=-\frac{1}{4\pi\epsilon_0}\frac{0.066}{d^3}\alpha^A\mu^B(d)\ ,$$
$$\mu_z^{A\leftarrow(a)}=-\frac{1}{4\pi\epsilon_0}\frac{0.102}{d^3}\alpha^A\mu^B(d)\ . \tag{29}$$

In order to discuss this result in the simplest possible way, we shall rewrite these results by inserting the constant η from Eq. (16). We get in units of cgs

$$\mu_x^{A\leftarrow(a)}=-0.025\frac{\alpha^A\eta^B}{d^7}\ ,$$
$$\mu_z^{A\leftarrow(a)}=-0.038\frac{\alpha^A\eta^B}{d^7}\ . \tag{30}$$

B. Depolarization of A by the static quadrupole induced on B by the surface

This second effect is represented by the graph in Fig. 4(B) [and all five others deduced from 4(b) by permuting vertices]. It can be calculated by using Refs. 6 and 7. As in the study of the first effect (presented in the above paragraph) the essential feature of the calculation is that integration over k' reduces the graph in Fig. 4(b) to its only "static" term. This can easily be interpreted by identifying a part of the graph in Fig. 4(b) with Fig. 3: The surface induces a quadrupole moment Q^B on the atom B; the static electric field of this quadrupole and of its image polarizes the atom A and thus creates a static dipole $\mu^{A\leftarrow(b)}$,

$$\mu_B^{A\leftarrow(b)}=\frac{1}{4\pi\epsilon_0}\sum_{\alpha,k,l}\tfrac{1}{3}Q_{kl}^B\partial_k^B[g_{\alpha l}^F(0,R_{AB})+\Theta_\alpha g_{\alpha l}^F(0,\tilde{R}_{AB})]\alpha_{\alpha\beta}^A(A)\ . \tag{31}$$

Making then use of Eqs. (2) and (25) and inserting the value of Q^B from (14) we obtain for spherically symmetric systems

$$\mu_x^{A\leftarrow(b)}=\frac{1}{4\pi\epsilon_0}\frac{1}{3}\alpha^AQ_{zz}^B\left[\frac{9}{X^4}+\frac{3X(X^2-16d^2)}{(X^2+4d^2)^{7/2}}\right]\ , \tag{32}$$

$$\mu_z^{A\leftarrow(b)}=\frac{1}{4\pi\epsilon_0}\frac{1}{3}\alpha^AQ_{zz}^B\left[-6d\frac{(3X^2-8d^2)}{(X^2+4d^2)^{7/2}}\right]\ . \tag{33}$$

In this last equation, we note that since X is always greater (or equal) than $2d$, the induced quadrupolar moment of adatom B depolarizes the adatom A.

If A and B are two identical atoms in contact with the surface and with one another, we obtain by using (28)

$$\mu_x^{A\rightarrow(b)}=+\frac{1}{4\pi\epsilon_0}\frac{171\times10^{-3}}{d^4}\alpha^AQ_{ZZ}^B\ , \tag{34}$$

$$\mu_z^{A\rightarrow(b)}=+\frac{1}{4\pi\epsilon_0}\frac{5.5\times10^{-3}}{d^4}\alpha^AQ_{ZZ}^B\ . \tag{35}$$

In order to later discuss this second process we shall rewrite these results by inserting Eq. (18); we find in cgs units

$$\mu_x^{A\leftarrow(b)}=-355\times10^{-5}\frac{e\alpha^A\alpha_Q^B}{d^7}\ , \tag{36}$$

$$\mu_z^{A\leftarrow(b)}=-11.5\times10^{-5}e\frac{\alpha^A\alpha_Q^B}{d^7}\ . \tag{37}$$

C. "Quantum contributions" to the dipole moment of A

As explained above, these effects correspond to the graph in Fig. 4(c) which is characterized by the impossibility of separating the interaction into two different physical processes acting on A and B, respectively. As far as we know, this effect has never been studied for adatoms. When permutating vertices in Fig. 4(c), there are two types of Feynman diagrams which appear. These are shown in Figs. 7(a) and 7(b). In the first, the atom B first absorbs the virtual photon emitted by A and there emits a second photon to come back into its initial state. In the second process, the act of emission by B precedes that of absorption of the initial virtual photon. One readily verifies using the rules we have derived in Refs. 6 and 16 to calculate such graphs, that the contribution of these two Feynman diagrams to ΔU is (taking into account all other permutations of vertices)

$$\Delta U_{(c)}=-\frac{1}{16\pi^2\epsilon_0^2}\frac{\hbar c}{6\pi}\sum_{i,j,k,l}\sum_{\alpha,\beta}E_l^s\int_0^\infty du\,\alpha_{\alpha\beta}^B(iu)\chi_{kl,ij}^A(0,iu)\times\{[g_{\beta k}^F(iu,R_{BA})+\Theta_\beta g_{\beta k}^F(iu,\tilde{R}_{BA})]\partial_i^A[g_{j\alpha}^F(iu,R_{AB})+\Theta_j g_{j\alpha}^F(iu,\tilde{R}_{AB})]+[g_{k\beta}^F(iu,R_{AB})+\Theta_k g_{k\beta}^F(iu,\tilde{R}_{AB})]\partial_i^A[g_{\alpha j}(iu,R_{BA})+\Theta_\alpha g_{\alpha j}^F(iu,\tilde{R}_{BA})]\}\ . \tag{38}$$

It is necessary to note the upper indice A in the differential operator ∂_i^A which indicates that the derivative is to be calculated for the components of the A position only in the expressions of R_{AB} and $\tilde{R}_{AB}$.

The expression (38) is very general and takes into account retardation effects. However, for adatoms, it will be sufficient to restrict the propagator to the nonretarded term [Eq. (11)]. Using then the following symmetry properties of g_{ij}^F:

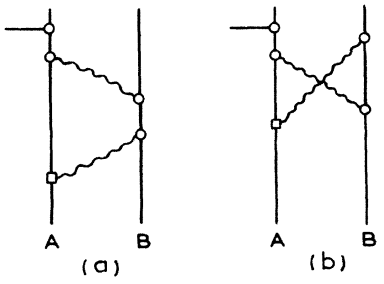

FIG. 7. Graphs illustrating the quantum contribution of system B on system A. (a) and (b) are the direct and crossed graphs which make the dynamical polarizability of system B appear.

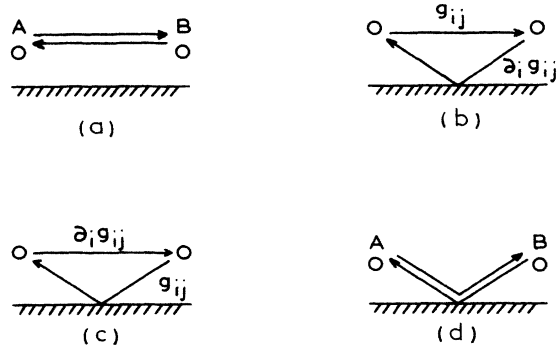

FIG. 8. Schematical representation of the exchange of virtual photons between the two adatoms. The dipolar or quadrupolar vertices can correspond to the direct or reflected part of the photon.

$$g_{\alpha\beta}(iu,R)=g_{\beta\alpha}(iu,R)\,,$$
$$\Theta_\alpha g_{\alpha\beta}(iu,\tilde{R}_{AB})=\Theta_\beta g_{\beta\alpha}(iu,\tilde{R}_{BA})\,, \tag{39}$$

Eq. (38) reduces (apart from a multiplicating factor of 2) to its only first term and can be written

$$\Delta U_{(c)}=-\frac{1}{16\pi^2\epsilon_0^2}\frac{\hbar c}{3\pi}$$
$$\times\sum_{i,j,k,l}\sum_{\alpha,\beta}E_l^s\int_0^\infty du\,\alpha_{\alpha\beta}^B(iu)\chi_{kl,ij}^A(0,iu)\left[\frac{1}{R^3}\left(\delta_{k\beta}-\frac{3R_kR_\beta}{R^2}\right)+\Theta_k\frac{1}{\tilde{R}^3}\left(\delta_{k\beta}-\frac{3\tilde{R}_k\tilde{R}_\beta}{\tilde{R}^2}\right)\right]$$
$$\times\partial_i^A\left[\frac{1}{R^3}\left(\delta_{j\alpha}-\frac{3R_jR_\alpha}{R^2}\right)+\Theta_j\frac{1}{\tilde{R}^3}\left(\delta_{j\alpha}-\frac{3\tilde{R}_j\tilde{R}_\alpha}{\tilde{R}^2}\right)\right]. \tag{40}$$

Four different processes appear in Eq. (40). The first term of the product (which is varying as R^{-7}) corresponds to the free field effect calculated for two atoms in vacuum.[27] The two following terms (varying as $R^{-3}\tilde{R}^{-4}$ and $R^{-4}\tilde{R}^{-3}$) are illustrated in Figs. 8(b) and 8(c): One of the two virtual photons mediating the interaction is directly exchanged between A and B; the other is reflected by the surface. In other words, system A is interacting both with B and its image. In the last term [Fig. 8(d)] the two photons are exchanged via the surface. By using Eq. (5) we obtain, in the case of two spherically symmetric systems located at the same distance d from the surface [we note in this case $l=\tilde{R}=(X^2+4d^2)^{1/2}$],

$$\mu_x^{A\leftarrow(c)}=\frac{1}{16\pi^2\epsilon_0^2}\frac{\hbar c}{2\pi}\int_0^\infty du\,\alpha_{zz}^B(iu)\chi_{zz,zz}^A(0,iu)\left[\frac{8}{X^7}-\frac{12}{l^3X^4}\left[\frac{d^2+X^2}{l^2}\right]+\frac{12}{l^4X^3}\frac{X}{l}\left[\frac{d^2-X^2}{l^2}\right]+\frac{18X}{l^8}\right] \tag{41}$$

(let us note that, when taking $d\to\infty$ we find the usual result for two atoms in vacuum[27]),

$$\mu_z^{A\leftarrow(c)}=\frac{1}{16\pi^2\epsilon_0^2}\frac{\hbar c}{2\pi}\int_0^\infty du\,\alpha_{zz}^B(iu)\chi_{zz,zz}^A(0,iu)\left[\frac{6}{l^4X^3}\frac{d}{l}\left[\frac{9X^2+4d^2}{l^2}\right]-\frac{36d}{l^8}\right]. \tag{42}$$

Although it is not the most concise form for $\mu_x^{A\leftarrow(c)}$ and $\mu_z^{A\leftarrow(c)}$, the above explanation has been used in order to clearly distinguish between the different contributions of processes 8(a), 8(b), 8(c), and 8(d) which appear in the same order as in results (41) and (42). In the case when A and B are two identical adatoms in contact both with one another and with the surface, we obtain, using Eq. (28) and keeping different processes 8(a), 8(b), 8(c), and 8(d) in the same order,

$$\mu_x^{A\leftarrow(c)}=\frac{1}{16\pi^2\epsilon_0^2}\frac{\hbar c}{2\pi}\left[\frac{18-2.65-0.79+1.125}{X^7}\right]$$
$$\times\int_0^\infty du\,\alpha_{zz}^B(iu)\chi_{zz,zz}^A(0,iu)$$
$$=\frac{1}{16\pi^2\epsilon_0^2}\frac{\hbar c}{2\pi}\frac{15.68}{X^7}\int_0^\infty du\,\alpha_{zz}^B(iu)\chi_{zz,zz}^A(0,iu)\,, \tag{43}$$

$$\mu_z^{A\leftarrow(c)}=\frac{1}{16\pi^2\epsilon_0^2}\frac{\hbar c}{2\pi}\frac{(1.85-1.12)}{X^7}\times\int_0^\infty du\,\alpha_{zz}^B(iu)\chi_{zz,zz}^A(0,iu)$$
$$=\frac{1}{16\pi^2\epsilon_0^2}\frac{\hbar c}{2\pi}\frac{0.73}{X^7}\int_0^\infty du\,\alpha_{zz}^B(iu)\chi_{zz,zz}^A(0,iu)\ . \tag{44}$$

In order to more easily estimate these terms it will be helpful to express them by using the $\overleftarrow{D}^7$ coefficient introduced by Byers Brown and Whisnant,[23]

$$\overleftarrow{D}^7=-\frac{9\hbar c}{\pi}\int_0^\infty du\,\alpha(iu)\chi(0,iu)\ . \tag{45}$$

We thus find

$$\mu_x^{A\leftarrow(c)}=-\frac{0.87}{(4\pi\epsilon_0)^2}\frac{\overleftarrow{D}^7}{X^7}\ , \tag{46}$$

$$\mu_z^{A\leftarrow(c)}=-\frac{0.04}{(4\pi\epsilon_0)^2}\frac{\overleftarrow{D}^7}{X^7}\ . \tag{47}$$

V. DISCUSSION

As explained above, three different processes contribute to the reduction of the permanent dipole induced by the surface on the atom. Our aim is now to estimate each of them. For obvious physical reasons we will only turn our attention to the z component of μ^A.

A. Contribution of the static dipole induced on B by the surface

This first term, given in Eqs. (27) and (30), can be compared with the permanent dipole μ^A [Eq. (17)] induced by the surface in absence of a neighbor. By using Eqs. (17) and (30) we can write (in cgs units)

$$\frac{\mu_z^{A\leftarrow(a)}}{\mu_z^A}=-0.1029\frac{\alpha^A}{d^3}\ . \tag{48}$$

Using then numerical values given by Standard and Certain[25] for the polarizability α of hydrogen atoms and of inert gases we find results presented in Table III.

In the particular case of Xe we obtain an idea of the relative importance of this effect with respect to the induced dipole moment μ_z^A by taking the distance d to be 2 Å, approximately the radius of the Xe atom. It becomes

$$\mu_z^{A\leftarrow(a)}/\mu_z^A\simeq 5\%\ . \tag{49}$$

Let us emphasize that these results correspond to the first term of the development of the consistent interaction of the permanent-induced dipole B on the atom A. On the other hand we have, in fact, only considered here one neighbor. For large coverage of the surface by the adatoms this classical reduction is of course more important (see, for instance, Topping[8]). The consideration of a more realistic surface will also explain the face specificity recently observed by Wandelt and Hulse.[28] However, this first process of depolarization will give the same order of magnitude.

B. Contribution of the static quadrupole Q^B induced on B the surface

The second process is illustrated by Fig. 4(b) and expressed in Eqs. (32), (33), (36), and (37). It can be compared with the value of $\mu_z^{A\leftarrow(a)}$ given in Eq. (30). Thus using Eqs. (15), (37), and (30) we obtain (in cgs units)

$$\frac{\mu_z^{A\leftarrow(b)}}{\mu_z^{A\leftarrow(a)}}=3\times10^{-3}e\frac{\alpha_Q^A}{\eta^A}\ . \tag{50}$$

This ratio can be estimated for each inert gas and for the hydrogen atom by using numerical values given by Byers Brown and Whisnant[23] for η (see also Table I) and by Standard and Certain[25] for α_Q. We thus obtain results presented in Table IV. By looking at Table IV, it becomes obvious that it is enough, for numerical estimates, to take $(\alpha_Q/\eta)\simeq 1$. We thus find that $\mu_z^{A\leftarrow(b)}\simeq 0.003\mu_z^{A\leftarrow(a)}$, and, consequently, the second process is always negligible compared to the first.

C. Contribution of quantum effects

The third process, presented in Sec. IV C, will be compared to the first. On using Eqs. (47) and (30) we can write

$$\frac{\mu_z^{A\leftarrow(c)}}{\mu_z^{A\leftarrow(a)}}=8.21\times10^{-3}\frac{\overleftarrow{D}^7}{\alpha^A\eta^B}\ . \tag{51}$$

TABLE III. Calculation of the relative dipolar depolarization $\mu_z^{A\leftarrow(a)}$ vs the permanent-induced dipolar moment μ_A. α is taken from Ref. 25 and the second column is calculated with (48).

	α (a.u.)	$(\mu_z^{A\leftarrow(a)}/\mu_z)d^3$ (a.u.)
H	4.5	−0.46
He	1.38	−0.14
Ne	2.66	−0.27
Ar	11	−1.13
Kr	16.7	−1.72
Xe	27	−2.78

TABLE IV. Numerical estimates of the relative quadrupolar depolarization. η is taken from Ref. 24 and α_Q from Ref. 25.

	η (a.u.)	α_Q (a.u.)	α_Q/η (a.u.)
H	16.5	15	0.91
He	2.52	2.44	0.966
Ne	8.62	6.42	0.745
Ar	39.2	50.21	1.28
Kr	73.06	95.55	1.30
Xe	(150)	212.6	(1.41)

TABLE V. Numerical estimates of the quantum depolarization. $\overleftarrow{D}^7$ and η are taken from Ref. 25.

	$\overleftarrow{D}^7$ (a.u.)	α (a.u.)	η (a.u.)	$\overleftarrow{D}^7/\alpha\eta$ (a.u.)
H	388	4.5	16.5	5.22
He	16.8	1.38	2.52	4.83
Ne	95.4	2.66	8.62	4.16
Ar	1698	11.1	39.21	3.90
Kr	4360	16.7	73.06	3.57

Calculations of this ratio can be made by using previous values for α and η after having estimated $\overleftarrow{D}^7$. This can be made by using the paper of Whisnant and Byers Brown,[24]

$$\overleftarrow{D}^7 = 6C^{\mathrm{I}}g^1 + 9C^{\mathrm{II}}g^2 . \tag{52}$$

Numerical results are presented in Table V. We thus see that quantum effects contribute to the reduction of the surface-induced dipole moment for about 3% of the contribution of the process (a). Although it can thus be neglected, it can be helpful to note that the last effect is more important than the second.

D. Final remarks

The complete quantum calculation presented in this paper clearly shows that the main process of depolarization of an adatom A by its neighbor B is a classical one which corresponds to the interaction between A and the static dipole induced on B by the surface. This justifies the use of the Topping's formula in a usual interpretation of experimental results.[29]

The recent paper by Wandelt and Hulse[28] on the adsorption of xenon on palladium shows that different dipole moments are obtained on the three low-index planes of palladium Pd(100), Pd(110), and Pd(111). To explain this it would be necessary to perform calculations based on a more realistic description of both the geometry of the surface and its physical structure. At this point the nonlinear characteristics of the surface as recently presented by Girard and Galatry[30] could have, at this same order of perturbation, an interesting influence on interactions between neighbors.

Lastly let us note that an effect of self-polarization of the adatom would be considered at this same fifth order of perturbation. The process illustrated by Fig. 9 can be calculated by using all the possible different diagrams obtained by permutating quadrupole and dipole vertices present in Fig. 9.

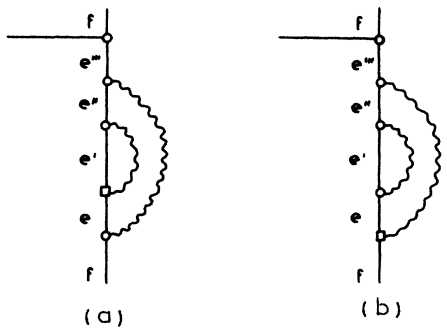

FIG. 9. Graphs illustrating the five-order perturbation term of the induced permanent dipole of the system A above. Some of the 60 different graphs correspond to the classical influence of the induced dipole (at the third order of perturbation) of A on the system A [e.g., (a)]. Some others correspond to the classical influence of induced quadrupole of A on system A [e.g., (b)].

Among these some 60 Feynman diagrams, those in which $|e''\rangle = |f\rangle$ will contribute to classical effects. It is to be expected that their contribution to the total self-polarization of the adatom will predominate and that they will increase the initial permanent-induced dipole of the atom. Among the classical effects we can distinguish between two different processes: The first one is illustrated by Fig. 9(a). Its physical meaning becomes clear when we identify (noting again that in this case $|e''\rangle = |f\rangle$) the graph of Fig. 2 as a part of the one of Fig. 9(a). This process thus corresponds to the self-polarization of the atom by the static electric field of its own permanent dipole. The other process, presented in Fig. 9(b) can be interpreted by analog considerations; it thus corresponds to the self-polarization of the atom by the static field of its own permanent-induced quadrupole. In the geometry of this present paper, the increase of the initial permanent dipole of the atom could be about 15% for the first effect for Fig. 9(a) and about 1% for Fig. 9(b).

ACKNOWLEDGMENT

The Laboratoire de Physique Moléculaire is "associé au Centre National de la Recherche Scientifique."

[1]P. R. Antoniewicz, Phys. Rev. Lett. **87**, 432 (1974).
[2]B. Linder and R. A. Kromhout, Phys. Rev. B **13**, 1532 (1976).
[3]R. A. Kromhout and B. Linder, Chem. Phys. Lett. **61**, 283 (1979).
[4]L. Galatry and C. Girard, Mol. Phys. **49**, 1085 (1983).
[5]L. Galatry and C. Girard, Chem. Phys. Lett. **101**, 242 (1983).
[6]Ph. Grossel, J. M. Vigoureux, and D. Van Labeke, Phys. Rev. A **28**, 524 (1983).
[7]Ph. Grossel, D. Van Labeke, and J. M. Vigoureux, Chem. Phys. Lett. **104**, 311 (1984).
[8]J. Topping, Proc. R. Soc. London, Ser. A **114**, 67 (1927).
[9]A. R. Miller, Proc. Cambridge Philos. Soc. **42**, 292 (1946).
[10]D. Van Labeke, Ph. Grossel, and J. M. Vigoureux, Chem. Phys. Lett. **109**, 598 (1984).

[11]D. Van Labeke, Ph. Grossel, and J. M. Vigoureux, Chem. Phys. Lett. **114**, 430 (1985).
[12]A. D. McLachlan, Mol. Phys. **7**, 381 (1964).
[13]M. Babiker, J. Phys. A **9**, 799 (1976).
[14]C. Mavroyannis, Mol. Phys. **6**, 593 (1963).
[15]M. Schmeits and A. A. Lucas, Prog. Surf. Sci. **14**, 1 (1983).
[16]Ph. Grossel, Thèse de Doctorat d'Etat, Reims, France, 1984 (unpublished).
[17]W. Kohn and L. J. Sham, Phys. Rev. **140A**, 1133 (1965).
[18]N. D. Lang, Phys. Rev. Lett. **46**, 842 (1981).
[19]B. Linder and R. A. Kromhout, J. Chem. Phys. **84**, 2753 (1986).
[20]K. L. C. Hunt, J. Chem. Phys. **80**, 393 (1984).
[21]L. W. Bruch and Th. W. Ruijgrok, Surf. Sci. **79**, 509 (1979).
[22]E. A. Power and T. Thirunamachandran, Phys. Rev. A **26**, 1800 (1982).
[23]W. Byers Brown and D. M. Whisnant, Mol. Phys. **25**, 1383 (1973).
[24]D. M. Whisnant and W. Byers Brown, Mol. Phys. **26**, 1105 (1973).
[25]J. M. Standard and P. R. Certain, J. Chem. Phys. **83**, 1985 (1985).
[26]O. Sinanoglu and K. S. Pitzer, J. Chem. Phys. **32**, 1279 (1960).
[27]J. M. Vigoureux, J. Chem. Phys. **79**, 2363 (1983).
[28]K. Wandelt and J. E. Hulse, J. Chem. Phys. **80**, 1340 (1984).
[29]P. W. Palmberg, Surf. Sci. **27**, 598 (1971).
[30]C. Girard and L. Galatry, J. Chem. Phys. **80**, 4553 (1984).